

Coastal vulnerability of a populated Arctic spit: A case study of Golovin, Alaska, USA

By

Jacquelyn R. Overbeck

Cherokee Nation Technology Solutions

600 4th Street South, St. Petersburg, Florida 33701

Formerly: University of Alaska Fairbanks, Department of Mining and Geological Engineering

P.O. Box 755800, Fairbanks, Alaska 99775

joverbeck@usgs.gov

Nicole E.M. Kinsman

State of Alaska, Division of Geological and Geophysical Surveys

3354 College Road, Fairbanks, Alaska 99709

nicole.kinsman@alaska.gov

Debasmita Misra

University of Alaska Fairbanks, Department of Mining and Geological Engineering

P.O. Box 755800, Fairbanks, Alaska 99775

dmisra@alaska.edu

ABSTRACT

Golovin, Alaska is situated on an Arctic spit subject to storm surge-induced geohazards from extratropical Pacific storms that regularly pass through the Bering Sea during fall storm seasons. Although generalized reports by the U.S. Army Corps of Engineers and the Government Accountability Office have found Golovin to be a priority action community for flooding and erosion, the localized assessment described here shows the shoreline to be dynamically stable with the highest potential for flooding on the lagoon side of the spit which is subjected to lower wave energy compared to the open ocean side. By incorporating long- and short-term morphologic measurements with nearshore numerical and empirically parameterized modeling, flooding and erosion are projected here for a range of 5- to 100-year storm return intervals. Flooding at Golovin is expected to be confined to the low wave-energy side of the spit during 5- and 10-year (recurrence interval) storms, with the 25-year storm identified as the most likely threshold event for overwash and flooding from the offshore direction. 50- to 100-year events are expected to overwash and flood from both sides of the spit. Golovin is less at risk from erosion than previous reports suggest which makes improved localized coastal geohazard assessments necessary for hazard mitigation design and management strategies, not only for Golovin, but other communities along the coast of Alaska that face similar geohazards.

A shallow coastal shelf along a coast aligned with extratropical Pacific storm tracks makes communities in northwest Alaska vulnerable to a wide array of coastal geohazards, including storm surge-induced flooding and erosion. Coastal flooding and erosion have become conspicuous civic and engineering issues in the region, drawing national awareness in the popular media. Although many generalized reports have identified communities as being threatened by flooding and erosion (U.S. Army Corps of Engineers 2009; U.S. General Accounting Office 2003;

U.S. Government Accountability Office 2009), the methods used to identify these hazards are not well documented. Minimal baseline data and quantification of these hazards has led to expensive and often experimental engineering solutions in this region, with mixed remediation success (Mason *et al.* 2012).

The proximal backshore of the coast generally consists of bluffs, berms, dunes, or anthropogenic structures (e.g. sea walls, revetments, etc.). These features act as buffers to storm-surge flooding and erosion and often serve as the first line of

ADDITIONAL KEYWORDS: Erosion, flooding, storm-impact, run-up, Digital Shoreline Analysis System, XBeach.

Manuscript submitted 13 July 2015, revised and accepted 9 October 2015.

defense for coastal infrastructure during extreme storm events. When total water levels (surge + astronomical tide + wave run-up) reach or exceed the elevation of proximal backshore features, sediment is transported to either the nearshore, inland, or offshore environment (Sallenger 2000), during specified storm-impact regimes (e.g. dune erosion/collision, overwash, and inundation) which may increase or lead to flooding of low-lying coastal infrastructure. Models have been built to replicate and predict these storm-driven morphologic changes, as well as total water levels at the shoreline, that range from empirically parameterized models to robust numerical models (e.g. XBeach and run-up parameterization; Roelvink *et al.* 2010; Stockdon *et al.* 2006). The objective of this study is to combine long- and short-term morphologic measurements with numerical and parameterized modeling to determine the vulnerability of a small Alaskan village, Golovin, to storm-surge flooding and erosion and to contribute relevant information for improving engineering solutions.

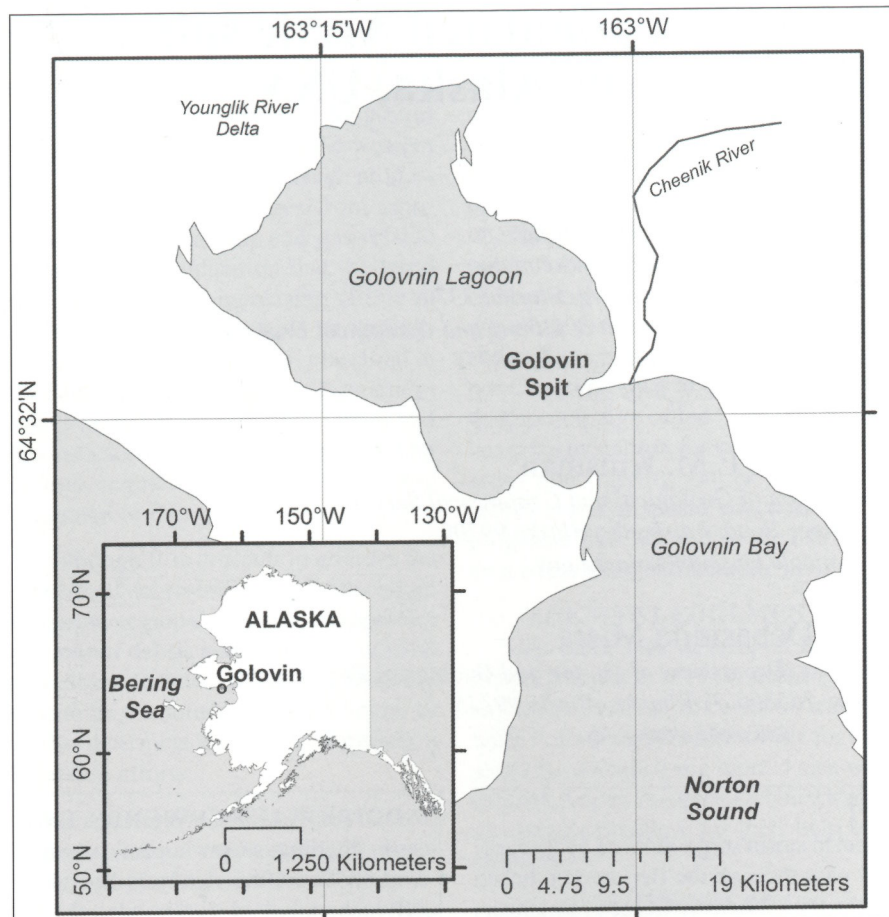


Figure 1. Regional map of Golovnin Bay and Lagoon relative to the Golovin Spit, and (subset) Golovin relative to the state of Alaska and the Bering Sea.

STUDY SITE

Golovin has been identified as a community imminently threatened by flooding and erosion (U.S. Army Corps of Engineers 2009; U.S. General Accounting Office 2003; U.S. Government Accountability Office 2009) and has been classified by the U.S. Army Corps of Engineers (USACE) as a priority action community for erosion problems (U.S. Army Corps of Engineers 2009). Golovin is home to 167 people, including members of the Chinik Eskimo community (Alaska Department of Commerce, Community, and Economic Development 2014). The majority of the residents reside on the Golovin spit at elevations below 10 m (relative to North American Vertical Datum of 1988 [NAVD88]), while new infrastructure is being built on an elevated bedrock surface at 30 m NAVD88 adjacent to the spit.

The Golovin spit is located along the northern coastline of Norton Sound in the Bering Sea, between Golovnin Bay to the south, and Golovnin Lagoon to the north (Figure 1). A spit and nearshore bar system protrudes from the western shoreline,

opposite and south of Golovin, which dissipates wave energy from Norton Sound. The tidal regime at Golovin is microtidal and diurnal. The Golovnin lagoon coastline is comprised of exposed bedrock shoreline, tundra, Yuonglik River delta sediments, as well as vegetated overwash and *Ivu* (ice push) deposits while the Golovnin Bay coastline is comprised predominantly of bedrock, bluffs, and vegetated overwash deposits. Golovnin Bay and Lagoon are both covered with sea ice during winter months. Although the time of freezing (November to December) and ice break-up (June to July) have remained consistent from 1853 to 2013, sea ice concentrations in the region have become more sporadic since the 1980s (Alaska Center for Climate Assessment and Policy and Scenarios Network for Alaska and Arctic Planning 2014). The ice-free season in the Bering Sea has been projected to increase from 5.5 to 8.5 months (Douglas 2010).

METHODS

Surveys of cross-shore elevation profiles, sediment characteristics, and water-levels were collected during field visits in

July 2012, July 2013, and October 2013. Aerial and satellite images of the study location acquired from 1972 to 2013 were used to determine long-term shoreline positions. Offshore storm-surge elevations and waves, modeled by the USACE (Chapman *et al.* 2009), for events with 5- to 100-year return intervals were used to force one-dimensional XBeach hydro-morphodynamic models and as inputs to a parameterized run-up model on the higher energy (bay) side of the spit (Profiles 1-5) to produce maximum total water elevations and erosion estimates.

Long-term shore positions

Historical rates of change at the upper beach were analyzed using the Digital Shoreline Analysis System (DSAS) toolbox for ArcGIS (Thieler *et al.* 2009). Seaward vegetation limits were manually digitized on five orthorectified and georeferenced aerial and satellite images (Table 1). The seaward limit of vegetation was used as a shoreline proxy rather than the mean high water line because of the lack of historical topographic and tidal data available in this region. Transects were cast perpendicular to the shorelines at 50 m alongshore spacing. A least-squares regression was performed on shoreline positions representing time periods between 1972 and 2013 for each transect. The linear regression rate-of-change was then derived from the annualized rate-of-change, weighted by the positional error of the shoreline at each time interval (E_p). For non-orthorectified products has been modified from Del Rio and Garcia (2014) using Equation 1.

$$E_p = \sqrt{G^2 + R^2 + C^2} \quad (1)$$

where G is the error due to georectification calculated by adding the sum-of-squares for errors produced by georeferencing the images to the 2004 orthorectified image (Table 1; RMS error) and the error of the orthorectified product (0.61 m), R is the error due to the spatial resolution of the image calculated as the sum-of-squares of pixel size of the image (Table 1; Ground Sampling Distance) and the error due to digitizing (2.4 m, calculated from digitizing the same line three times and determining the average distance between lines), and C is the error due to large changes in elevation near the shoreline, which were assumed to be zero.

Beach sediments

Both physical and image-based surface sediment samples were taken in the

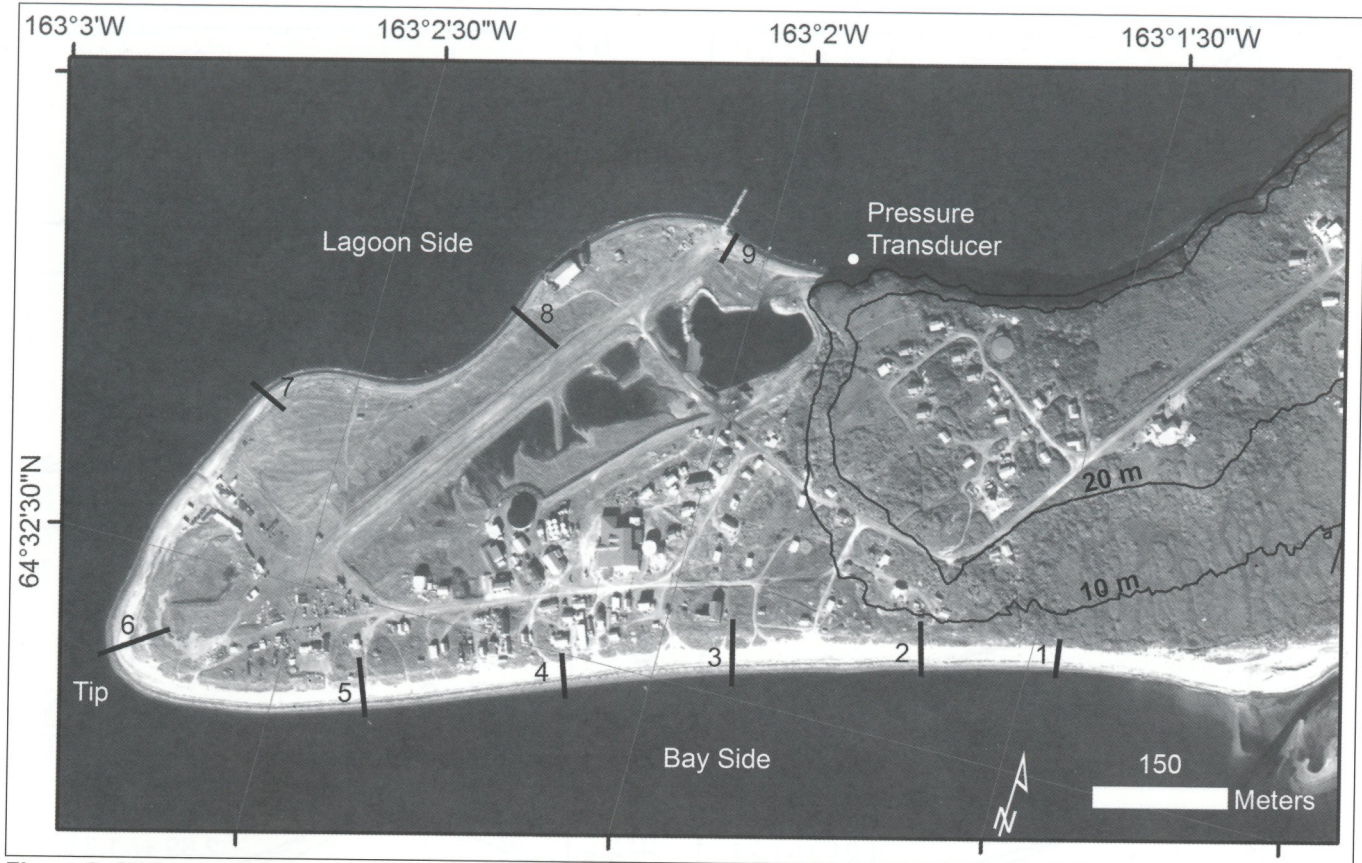


Figure 2. GPS-measured cross-shore profiles on the Golovin spit. The bay side, tip and lagoon side are labelled, as well as the location of the pressure transducer. Elevation contours are delineated for 10 m and 20 m NAVD88.

field to determine cross-shore grain size. The physical samples (taken at Profiles 2, 5, 7, and 9) were used to verify the accuracy of the image-based samples. Image-based samples were taken at grain size transitions, resulting in 3-6 samples per survey transect. Cumulative grain size distributions were measured by sieving the physical samples and using an image autocorrelation algorithm on the image-based samples (Buscombe *et al.* 2010; Warrick *et al.* 2009). Cross-shore measurements of D_{50} and D_{90} were averaged and used for inputs into the XBeach models (Table 2). Sediments were analyzed visually for composition and comparison to surrounding bedrock features.

Elevations and model domains

Cross-shore beach and berm elevation profiles were measured using RTK-GPS (Top Con HiPerII) and re-occupied during each of the field excursions (Figure 2; July 2012, July 2013, and October 2013). Measured elevations were post-processed with (Top Con) Tools software. Vertical precision of the survey ranged from 0.40-0.65 cm, with 0.11-1.10 cm corresponding horizontal precision. Sub-aerial unit profile volume was computed

Table 1. Datasets used in digital shoreline analysis

Acquisition date	Image source	Type	Ground sampling distance (m)	RMS error (m)	Ep (m)
8/1/1972	USGS ¹	Aerial photography	4.50	1.31	5.30
7/1/1980	AHAP ²	Aerial photography	1.66	0.58	3.03
6/11/2004	DCCED ³	Aerial photography	0.61	0.61	2.61
9/9/2009	SPOT5 ⁴	Multispectral satellite imagery	2.50	0.88	3.62
9/17/2013	Worldview-2 ⁵	Panchromatic satellite imagery	0.50	0.30	2.53

¹U.S. Geological Survey.

²Alaska High Altitude Photography.

³Alaska Department of Commerce, Community and Economic, Development.

⁴Satellite Pour l'Observation de la Terre 5.

⁵Digital Globe, WorldView2 satellite imagery.

as the area under the measured profile within the spatial bounds shared by the profiles, which included beach and proximal backshore volumes (assuming a 1 m wide profile). Beach slopes were measured by taking the average slope between each measured point along the cross-shore profile from the swash zone to the berm toe.

One-dimensional grids for the XBeach models were created using surveyed elevations and the best data layer for bathymetric depths. The bathymetry was derived from the spectral response measured in WorldView-2 multispectral imagery over Golovin Bay and Lagoon, calibrated to single-beam sonar measurements made in July 2012 (Smith 2014;

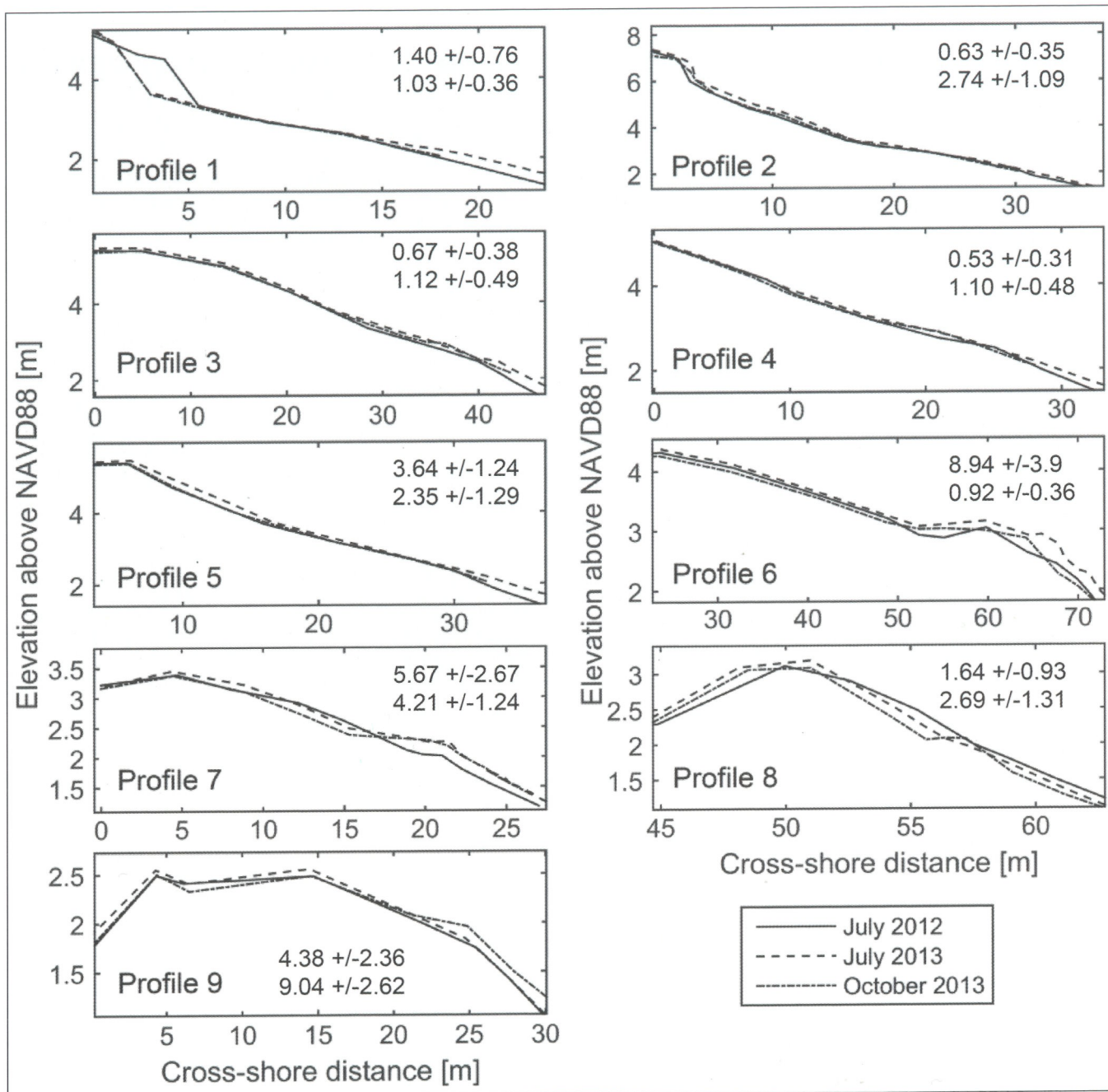


Figure 3. RTK-GPS measured profiles from July 2012, July 2013, and October 2013, offshore is to the right. Mean grain size (mm) of the swash zone is shown in each panel for July 2012 (upper) and July 2013 (lower) +/- one standard deviation.

Table 2.
XBeach grain size parameter inputs at modeled profiles 1-5

Profile	D50 (mm)	D90 (mm)
1	1.30	1.44
2	2.50	4.03
3	1.52	2.63
4	1.96	3.30
5	3.94	6.44

Smith *et al.* 2013). The model profiles were extrapolated perpendicular to the shoreline to the 20 m isobath. Irregular grid spacing was used, with increased distance between grid nodes in the offshore direction.

Hydrodynamics

Water-level data were collected using a Solinst pressure transducer from July 2012 to October 2012. An atmospheric correction was applied based on the measured atmospheric pressure at the local airport (approximately 7.2 m above

MTL; Iowa State University of Science and Technology 2013). To calculate the local tidal datum and range, the corrected water level time series was evaluated using a Matlab algorithm (Pawlowicz *et al.* 2002) to interpret major tidal constituents. The MTL was 1.28 m above NAVD88, with a diurnal tidal range of 0.43 m. Astronomical tide effects were not included in the XBeach model hydrodynamics, because of the low tidal amplitude and unknown timing throughout the duration of any given storm.

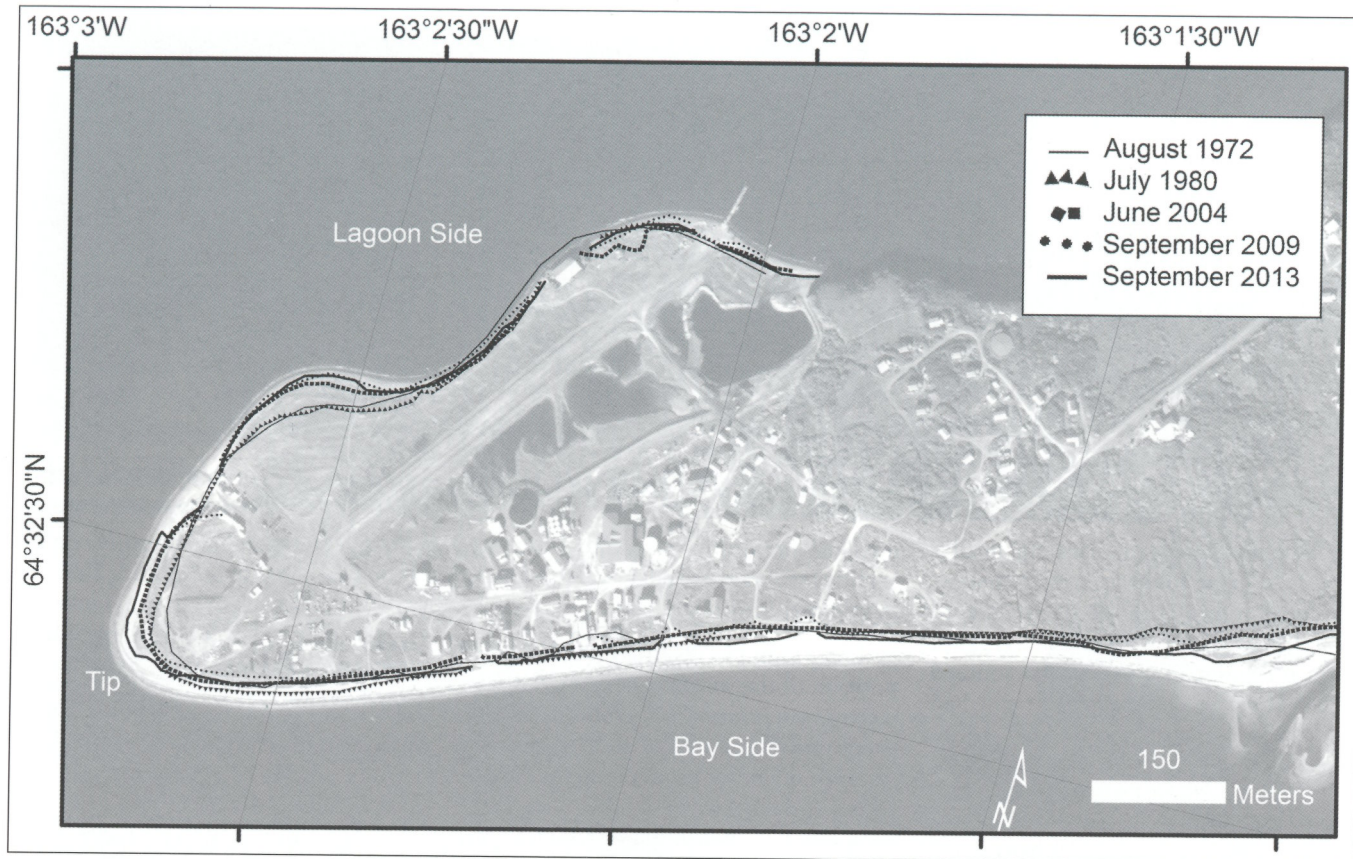


Figure 4. Vegetation lines delineated on aerial and satellite imagery from 1972-2013, on panchromatic WorldView-2 image.

The USACE developed a series of region-wide advanced circulation models for oceanic, coastal and estuarine waters (ADCIRC; Chapman *et al.* 2009), to determine offshore elevations of storm surge at different return intervals (5-, 10-, 25-, 50- and 100-years; Table 3) for the western coast of Alaska, including Golovin. The offshore surge elevations were used to drive storm surge in the XBeach models created during this research. Wind, and therefore, wind-driven-wave direction were taken as the weighted averaged from the 10 storms with the highest storm surge elevations (191.25° from north; Chapman *et al.* 2009), since wind direction was not related to storm surge elevation for those storms.

Maximum significant wave heights, for the same return intervals, were derived from the Wave Information Studies website, also developed by the USACE using the WAM Cycle 4.5 wave model (U.S. Army Corps of Engineers 2013). Each of the return intervals used to determine storm water elevations were used in the wave height-return period relationship at WIS station 82124 (U.S. Army Corps of Engineers 2013), to calculate the maximum significant wave heights

Table 3. Empirical and model derived hydrodynamics

Return interval (years)	Surge (m) ¹	Significant wave height (m) ²	Wind speed (m/s) ¹	Peak wave period (s) ³
5	1.83	3.71	13.15	9.71
10	2.44	4.12	13.90	10.20
25	2.99	4.66	14.75	10.87
50	3.68	5.08	15.40	11.36
100	4.46	5.50	16.03	11.76

¹ Chapman *et al.* (2009).

² U.S. Army Corps of Engineers (2013).

³ Sorensen (2006)

for the modeled storm events offshore of Golovin (Table 3). Peirson-Moskowitz parameters for wind velocity and peak wave frequency were then calculated from the significant wave height (Sorensen 2006). The resulting significant wave heights and frequencies were assumed to be representative of the Joint North Sea Wave Project (JONSWAP) spectrum and used to force the XBeach models.

Another common method for determining total water levels on the beach is to use an empirically parameterized relationship. The Stockdon *et al.* (2006) method for determining wave run-up

is widely used, and requires only wave height and period at the 20 m isobath, and beach slope as input parameters. The parameterized run-up elevation was added to projected surge elevations to compare with the XBeach-derived total water levels at the shoreline.

RESULTS

Morphologic trends

The Golovin spit is composed of very fine sand to medium gravel, with a mean grain size of 2.72 mm (+/- 0.68 mm standard error). The bedrock cliffs composed of monzonite-syenite to the south and schist to the north of Golovin both contribute to sediment composition

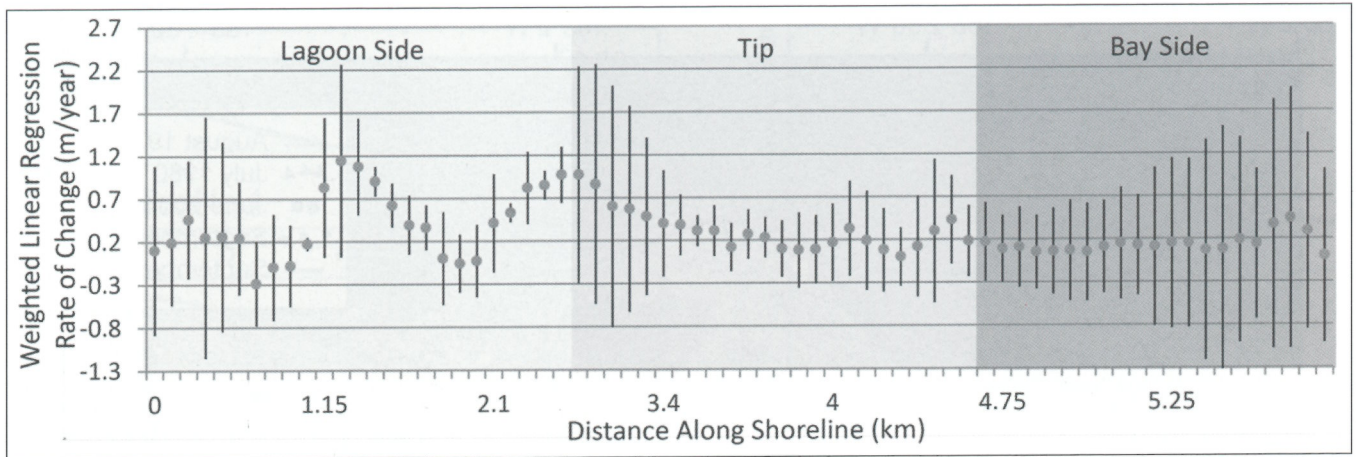


Figure 5. Weighted linear regression rates of shoreline change at every 50 m alongshore shown as gray circles, with the 95% confidence interval shown as a black line.

on the spit, with grain sizes suggesting selective rates of longshore transport due to littoral drift. Grain size increased near the Cheenik River outlet (Figure 3) suggesting sediment is also sourced from the river. The tip of the spit had slightly larger grain sizes, likely due to increased wave energy near the channel into Golovnin Lagoon. The grain size distributions around the Golovin spit were fine-skewed, very platykurtic, with moderate sorting, which is atypical of common beach sediments. This suggests a lack of hydraulic forcing on most portions of the beach face, which could be due to low tidal and wave energy for extended periods. The presence of landfast sea ice during large portions of the year would reduce the amount of wave energy reaching the beach while

the close proximity of sediment sources supplies sediments that have been subject to minimal reworking.

Long-term (1972-2013) trends in the position of the seaward vegetation limit were bi-directional on an inter-annual timescale (Figure 4). The greatest observed net shoreline movement was at the tip and northwestern lobe of the spit, with smaller measureable changes on the bay side and minimal changes on the sheltered (lagoon) side (Table 4). The most seaward position of the shoreline was in September 2013 for most locations around the spit (Figure 4). The weighted linear regression of shoreline change followed a similar pattern, with the greatest average rates on the tip of the spit, positive and negative on the bay side

of the spit and marginally positive on the lagoon side of the spit (Figure 5; Table 4). The rates of shoreline change, however, were on the same order of magnitude as the annualized error (0.19 m/year).

Changes to the beach volume and slope were measured at the cross-shore profiles surveyed on an annual and seasonal time interval (Table 5; Figure 3). Beach volume was reduced from the summer to the fall profile, except for Profile 2, in which beach volume increased. Profile 1 decreased in volume from July 2012 to July 2013, with an associated increase in beach width. Erosion was observed at the vegetation line of Profile 1 (Figure 6), where an abandoned municipal water supply pipe was transported from the berm to the beach

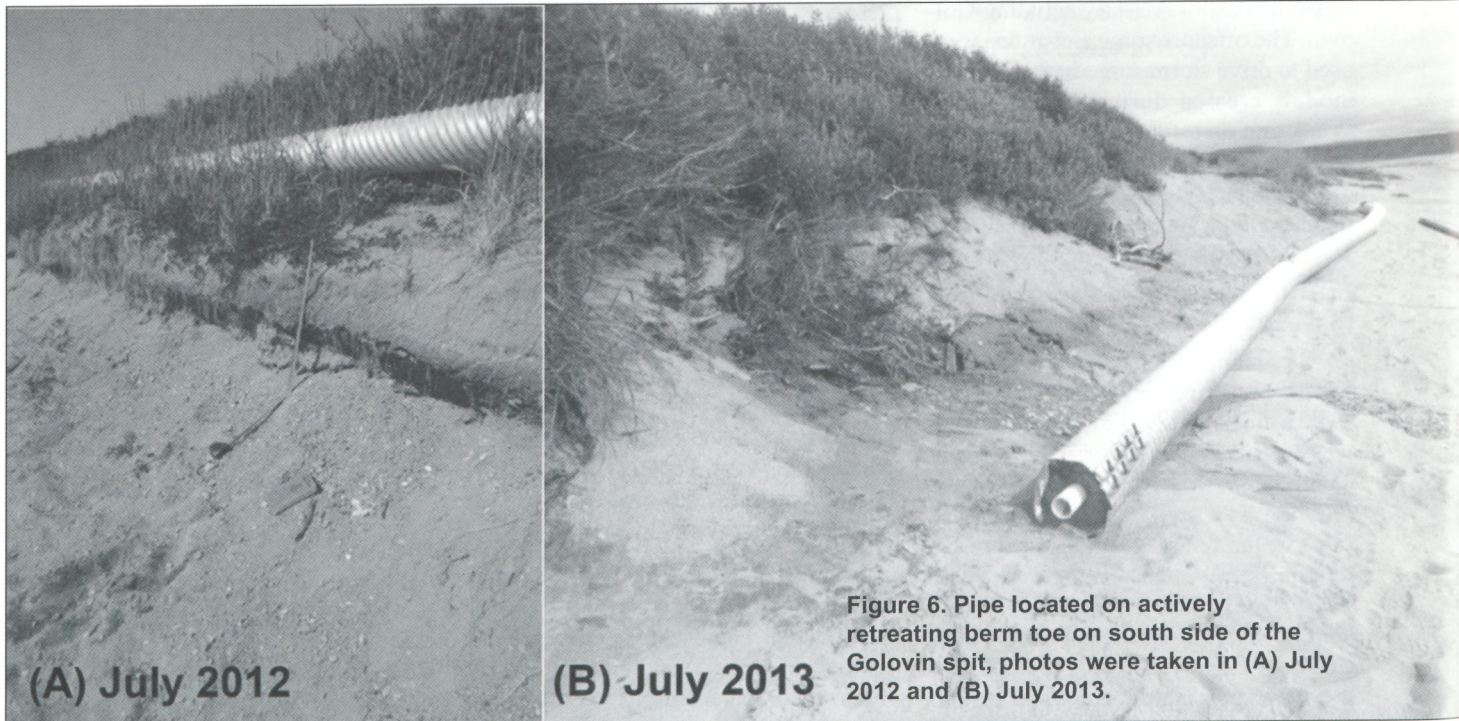


Figure 6. Pipe located on actively retreating berm toe on south side of the Golovin spit, photos were taken in (A) July 2012 and (B) July 2013.

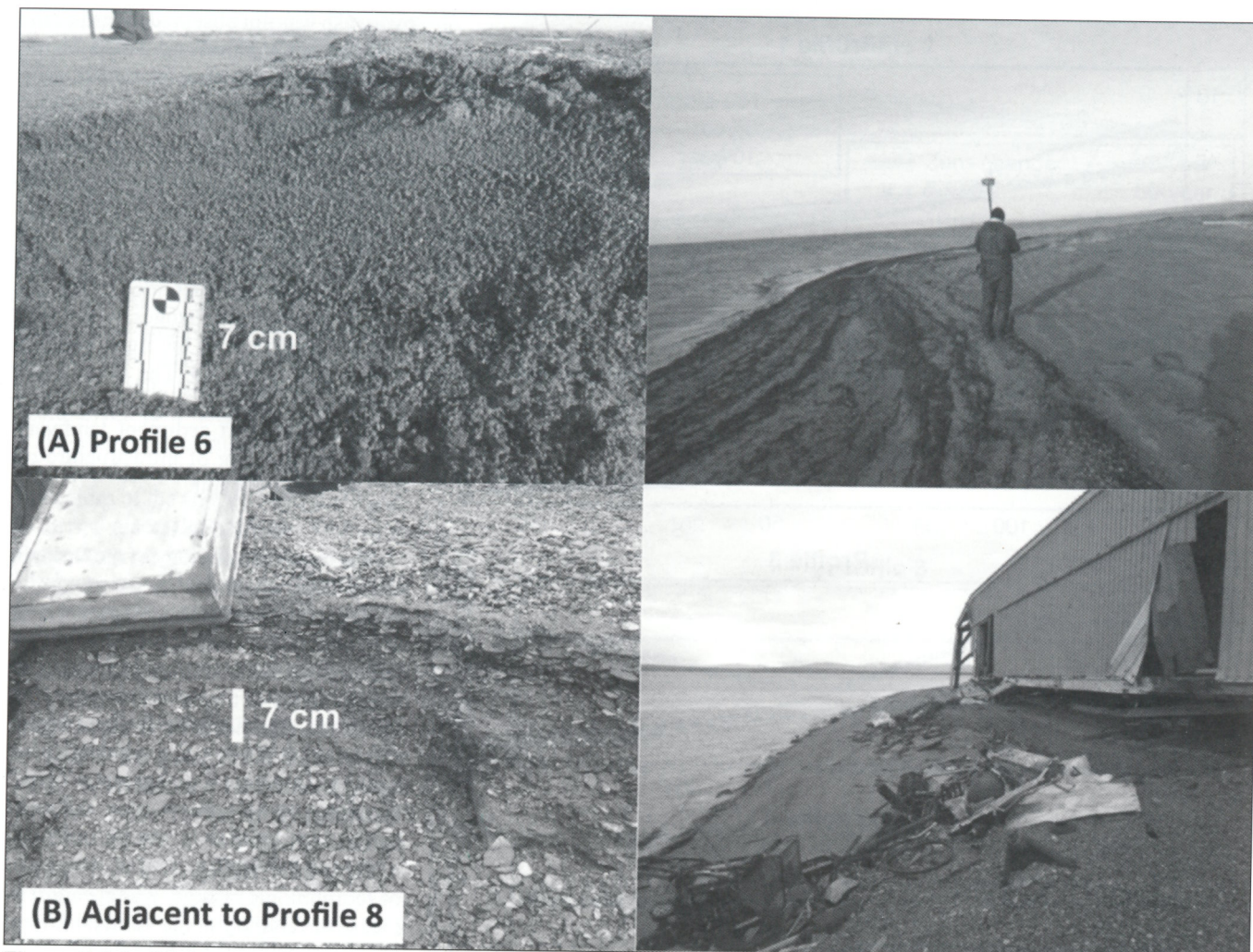


Figure 7. Intertidal scarps formed during October 2013 on (A) the tip of spit at Profile 6 and (B) on the lagoon side of the spit near Profile 8.

surface between July 2012 and July 2013. These changes in profile volume suggest permanent, rather than seasonal erosion at Profile 1. Profiles 2-5 and 9 experienced volume increases and reductions in beach slope from July 2012 to July 2013, which is consistent with the prograding shoreline. While Profiles 6-7 experienced volume increases and beach steepening.

Profiles 6 and 8 lost beach volume from summer to fall and also had intertidal scarping (Figure 7), typical of seasonal, recoverable changes in beaches as wave energy decreases in the summer. Profile 5 experienced a large seasonal change in beach width and volume, and was the only profile on the south side of Golovin to experience a large seasonal loss, which may have occurred because of the location of Profile 5 near the tip of the spit. Seasonal beach volume envelopes were on average of 0.4 m³ for the bay side, 14.3 m³ for the tip, and 3.0 m³ for the lagoon side. Seasonal changes from July to October 2013 were smaller than

Table 4.
Shoreline change trends from 1972 to 2013

Location on spit	Net shoreline movement (m)	Average rates of shoreline change (m/yr)	Range of rates of shoreline change (m/yr)
Bay side	0-15	0.32	-0.29-1.14
Tip	35-55	0.60	0.31-0.97
Lagoon side	15-35	0.16	0-0.44

the annual changes, however, most beach slopes were still reduced (Table 5). Beach slope, volume, and shoreline change were found to have the greatest envelopes of change on the tip of the spit, with minimal changes on the bay side, and minimally positive on the lagoon side.

Model results

The five storm events, representing typical storms of 5- to 100-year return intervals, were run for five XBeach model domains and used to predict flooding and subsequent morphologic changes to the beach and berm systems on the Golovin spit. Model results indicate the

three profiles backed by low elevations (Profiles 3-5) experienced berm erosion at the 5- and 10-year return interval conditions, with minimal overwash at the 25-year return interval and extreme overwash and flooding at the 50- and 100-year return interval conditions (Figure 8). Erosion at the vegetation line increased at these locations until the 50-year storm, which was similar to the 100-year storm (Figure 9). This suggests that erosion rates are maximized at the 50-year return interval. For Profiles 1-2 which were backed by higher elevations, erosion near the vegetation line continued to increase with increased storm return interval, and

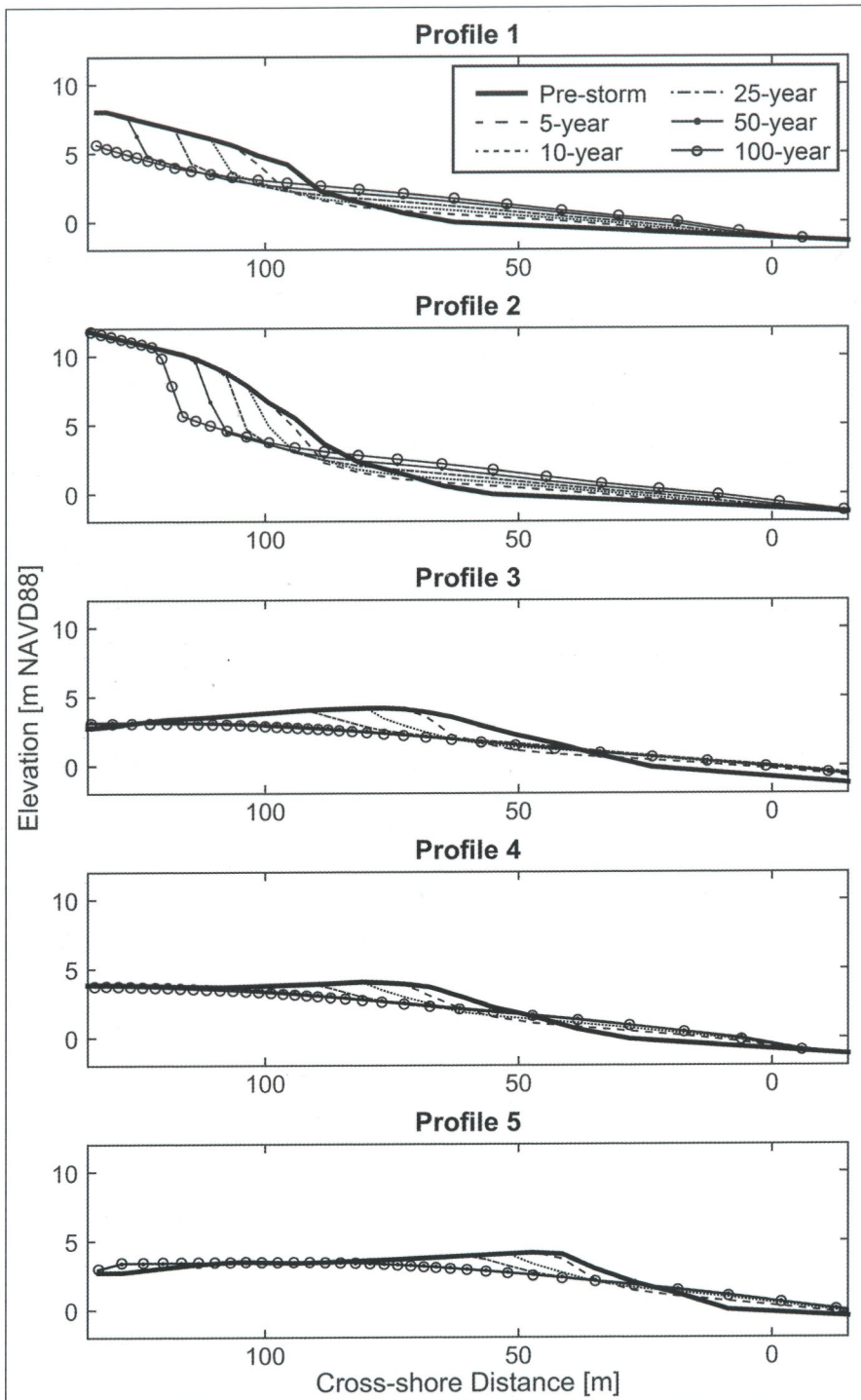


Figure 8. Morphologic responses of XBeach models at Profiles 1-5 to storm hydrodynamics ranging from 5-100 year return intervals, erosion of the berm is increased with increasing return interval. Offshore is to the right.

overwash was not observed. Much of the sediment eroded from all of the berms was transported to a nearshore bar.

Maximum run-up was modeled using both XBeach and empirical parametrization. The results varied at each profile location (Figure 10), with the empirical method generally exceeding the XBeach models. Maximum run-up from the XBeach model corresponded to the observed morphologic changes, where Profiles 3-5 experienced the most extreme erosion and overwash. The lower berm elevations at these profiles allow water levels to transport sediment landward and cause flooding of infrastructure on the low-elevation spit.

DISCUSSION

The beach morphology of the Golovin spit is likely dominated by the proximity of sediment sources rather than wave or tidal energy. Because the rates of shoreline change were minimal and ranged from positive to negative along the spit, there is no significant trend of erosion or accretion for the 41 year period analyzed here; the shoreline is dynamically stable, experiencing episodic erosion followed by sediment accretion. The tip and lobes of the spit had higher seasonal envelopes of morphologic change, which could increase uncertainty of the vulnerability to erosion and flooding at these locations. If a storm were to pass over Golovin during a time of low beach volume and higher beach slopes, the spit would be more vulnerable to erosion and flooding. Reduced beach volume would provide a smaller buffer to beach erosion and steeper beach slopes enhance wave run-up elevation and extent. Because the current morphology of the Golovin beaches are maintained in part due to protection from wave forcing by sea ice, longer ice-free seasons in the Bering Sea may expand the net beach change envelope, making the spit more susceptible to flooding and erosion from future storms.

Flooding along the bay side of the Golovin spit was modeled using multiple methods. To determine a single elevation of total water level for each return interval, the alongshore values of parameterized and numerically modeled total water levels were combined and averaged (Figure 11). A 95% confidence interval was then calculated for each return interval to provide a measure of uncertainty (Figure 11). When the mean total water levels

are projected onto a digital elevation model of the spit (Southernland and Kinsman 2014), the potential for flooding of infrastructure becomes apparent (Figure 12). The < 10-year storms are shown to flood large portions of the spit; however, minimal infrastructure is affected. All of the flooding occurs from the lagoon side of the spit, where lower elevations and the potential for ebb flooding are greatest. Wave energy on this side of the spit, however, would be minimal compared to the bay side, making an unconsolidated levee a viable mitigation structure in comparison to a hardened structure for < 10-year return interval storms. The 25-year storm results in flooding from both sides of the spit, through small gaps in berms along the bay side. This surge recurrence interval, however, is similar to observations made in the 2011 Bering Sea Storm (Kinsman and DeRaps 2012; Figure 12). High-water marks measured after the 2011 storm, from the bay side of the spit, correspond to the 25-year surge level (Figure 11), but there was no overwash during the 2011 event. The 25-year storm may be a threshold event that, due to uncertainties in alongshore elevations of total water level, may or may not result in flooding from the bay side of the spit. Small changes in berm heights or filling in of overwash pathways may reduce the potential for flooding during the 25-year storm. The > 50-year storms have high enough water levels to induce overwash and flooding from both the bay and lagoon sides of the spit.

During the 2011 Bering Sea Storm, extreme flooding on the lagoon side of the spit was avoided due to a locally led construction project that increased the elevation of a road (Antone Street; Figure 12). A minor increase in the road elevation was able to protect the inland depression in the middle of the spit where a majority of the local infrastructure exists. A storm of unknown return interval passed over Golovin during fall of 2013. The localized response was to build a temporary berm of unconsolidated materials (approximate location in Figure 12; example in Figure 13). The berm performed adequately to diminish flooding of the Golovin spit. Temporarily built berms have been shown to perform well in other scenarios as well, providing a larger buffer to the backshore coastal system during extreme events (Sanders *et al.* 2013) without permanently hardening the shoreline.

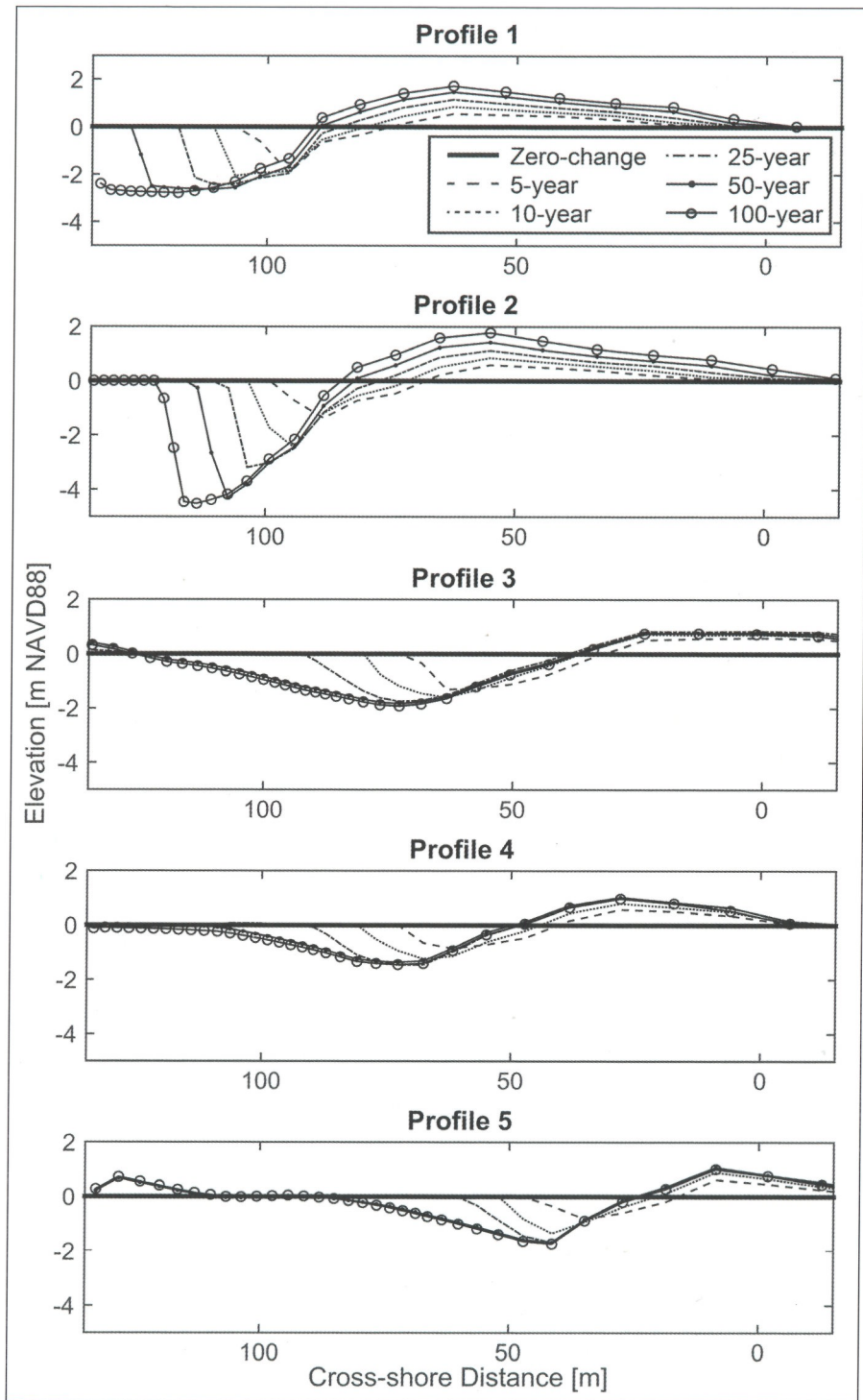


Figure 9. XBeach modeled elevation changes for Profiles 1-5, positive elevation change is accretion, while negative elevation change is erosion, erosion increases with increased storm return interval. Offshore is to right.

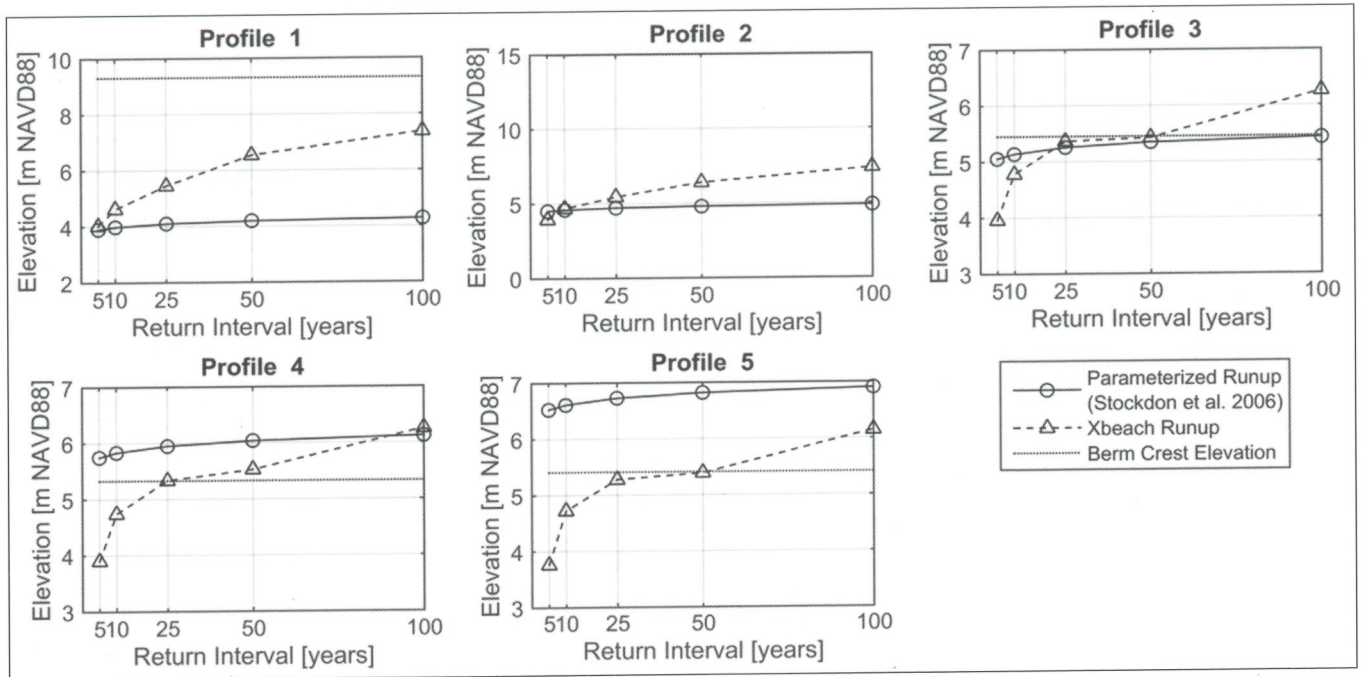


Figure 10. Maximum runup at Profiles 1-5 using the parameterized model and XBeach model. The black line shows the location of the berm crest for each profile, indicating that if water levels exceed the berm crest, overwash and/or overtopping may occur.

Table 5.
Annual and seasonal changes to beach morphology

Profile	Average summer change in slope (m/m)	Annual change in slope (%) (7/2012-7/2013)	Seasonal change in slope (%) (7/2013-10/2013)	Annual change in volume m ³ (7/2012-7/2013)	Seasonal change in volume m ³ (7/2013-10/2013)
1	0.110	-10.8	-4.3	-1.63	-0.77
2	0.133	-13.9	-0.2	4.70	3.79
3	0.105	-7.1	-13.1	4.46	-2.95
4	0.115	-8.6	+1.5	1.46	-1.67
5	0.120	-12.1	-3.5	3.08	-19.0
6	0.120	53.0	-21.6	7.29	-9.63
7	0.130	30.4	16.4	2.24	-1.76
8	0.160	16.1	-21.0	3.12	-7.07
9	0.110	-2.3	-16.4	1.65	-0.19

The modeled values of erosion and maximum total water levels may be unrealistically high in the model environment because of the potential effects of snow and ice. Fall storms often occur during frozen beach conditions with ice slush in the nearshore and open ocean (e.g. the Bering Sea Storm 2011; Figure 14). Frozen beach conditions would likely reduce erosion of the beach face during storm events, because of increased material strength provided by the ice. However, a smoother beach surface would also reduce friction in the swash zone, which may increase run-up. Sea ice and slush dampen wind generated waves in the open ocean and nearshore and would reduce maximum wave heights reaching

the beach. Without a better understanding of these mechanics, we cannot model storm surge impacts on the frozen coast using XBeach.

The resulting estimations of maximum run-up were dependent on modeled outputs from the USACE. Predictions were made using 16 years of water-level data available at the Nome tide station (Chapman *et al.* 2009). Since the water-level record did not extend to the highest return interval frequency analyzed here, some error may have been propagated into the hind-casted extrapolation of the 25-, 50-, and 100-year storms, resulting in overestimation of maximum run-up elevations. Sea-level rise, however, was not included in the USACE model used in this re-

search, which may increase storm-surge water levels at higher return intervals. The results of the modeling completed in this study were similar to values modeled for Shaktoolik, Alaska, where overwash of the Shaktoolik spit was expected at the 50-year return interval (U.S. Army Corps of Engineers 2011). Errors in long-term hind-casting extrapolation may lead to over-engineering structures if the people of Golovin choose to build a flood diversion structure. These same issues may arise for many other communities in Northwest Alaska facing similar geohazards.

The parameterized run-up elevations were higher than the XBeach modeled elevations. This may be due to the effects of the large nearshore bar that breaks wave energy during extreme storms; the nearshore environment is not considered in the parameterized model. However, using multiple methods of determining run-up along the coastline is best for providing uncertainties in maximum total water elevations.

CONCLUSIONS

Golovin, like and unlike other communities throughout Alaska, has been ranked as at risk to flooding and erosion. However, our results show that Golovin may be less at risk to erosion than indicated by previous studies, due to the dynamically stable shoreline through a 41-year period. The modeled erosion due to storm events

was found to be extreme, but contained only to the nearshore environment for the <10-year storm elevations, which would allow for beach recovery during calmer conditions. Extreme water levels for the <10-year events are expected to cause flooding from the sheltered side of the spit, making an unconsolidated flood control structure a viable option for flood protection. The 25-year storm may also be mitigated by an unconsolidated berm, if small depressed locations are also filled to protect from flooding on the exposed side of the spit. Model results for the >50-year storms caused overwash of beach sediments and flooding from both sides of the spit, however, results may have been distorted by projection of long return intervals without having enough data for validation. The models used here rely on sound field investigation for model construction; however, challenges are compounded when models do not account for processes like the attenuation of wind and wave energy by sea ice, increased material strength of a frozen coast, and reduced shear stresses of the frozen coast effects on wave run-up. Efforts have been made to minimize these errors by using multiple methods of determining wave run-up while considering alongshore variability in flooding.

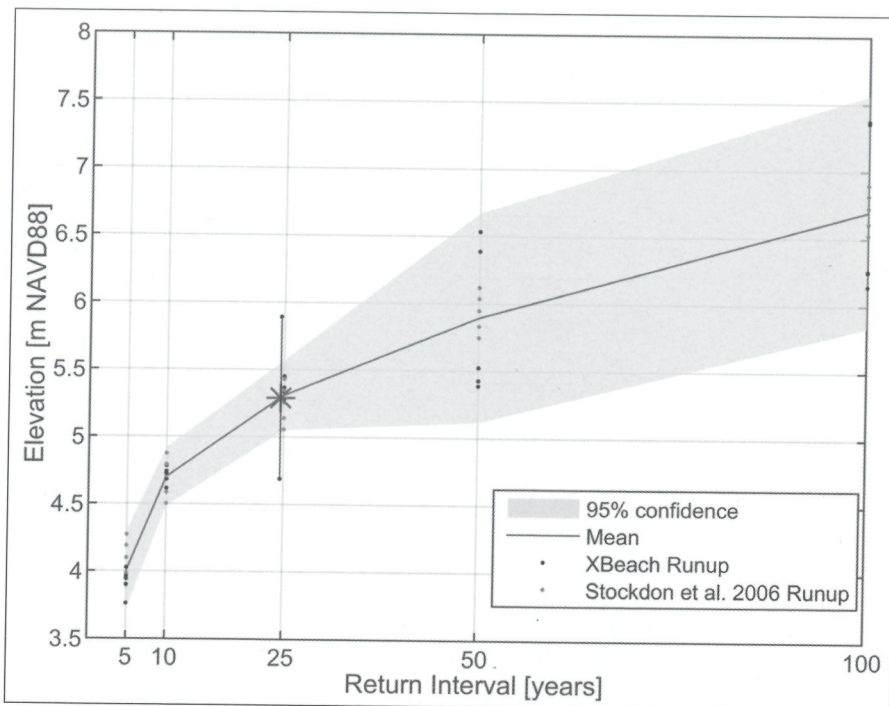


Figure 11. Total water level predictions for the Golovin Spit, using alongshore variable runup elevations from Stockdon et al. (2006) and XBeach models to derive mean and 95% confidence of flooding elevations. Asterisk and black error line show a measured storm event from the Bering Sea Storm in November 2011.

Figure 12. Flood extents for different storm return intervals delineated on digital elevation model (Southerland and Kinsman 2014) along with the flooding extent measured after the 2011 Bering Sea Storm (Kinsman and DeRaps 2012).

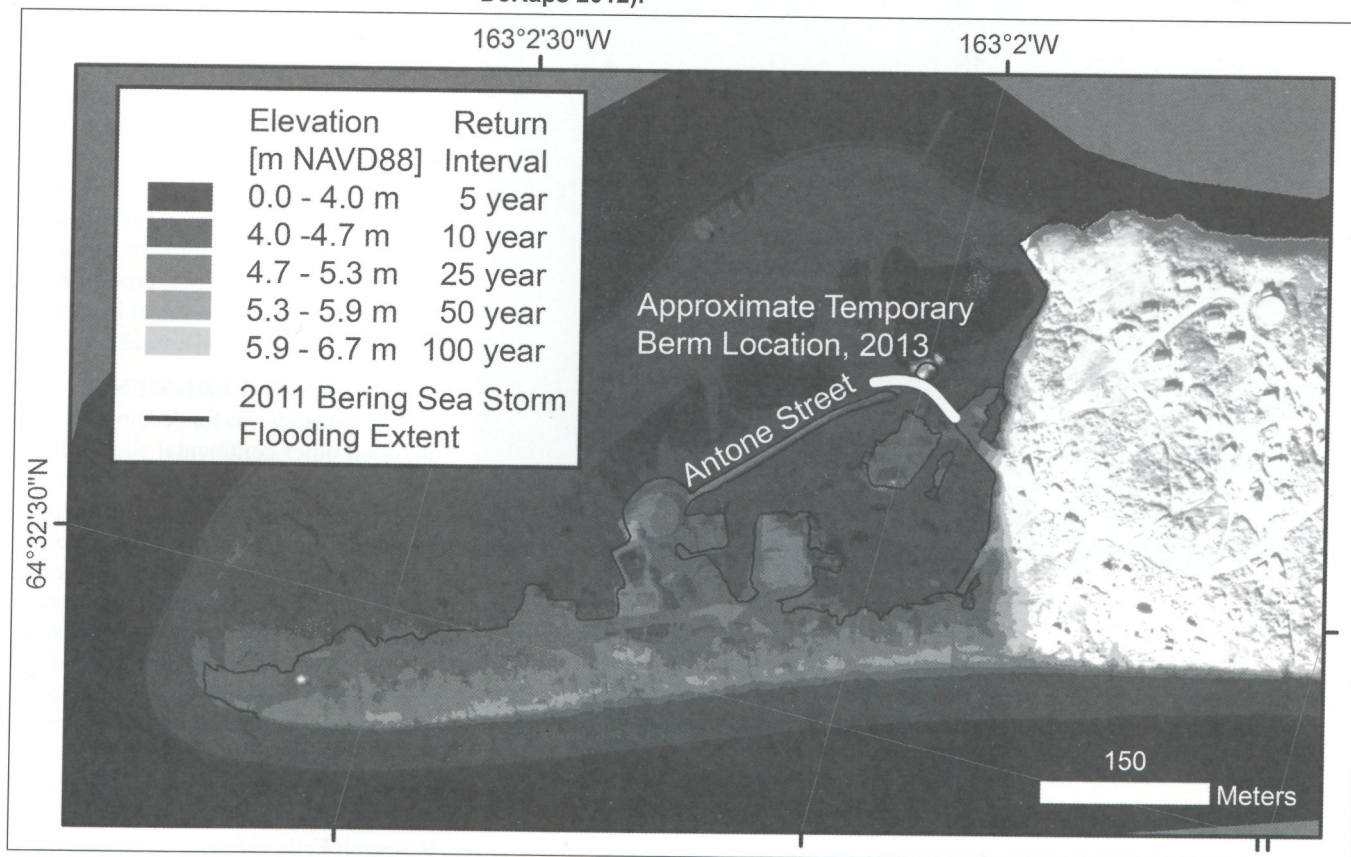




Figure 13. Temporary unconsolidated berm connected to Antone Street, built during local effort to reduce flooding from an incoming storm in fall 2013, berm and storm elevations are unknown. Frozen floodwaters are shown on the right (lagoon side of the spit) with minimal to no flooding observed on the left.



Figure 14. Frozen slush deposited by November 2011 Bering Sea Storm on bay side of spit.

Site-specific vulnerabilities need to be considered to effectively assess statewide geohazards, rather than generalizations to address social and engineered mitigation. Locally-led efforts to mitigate erosion and flooding are valuable engineering strategies. Local knowledge about extreme events combined with storm-response temporary berm construction may mitigate flooding on a storm-by-storm basis rather than a stationary hardened structure that may increase erodibility of the beach and cause financial burden on local, state, and federal entities.

ACKNOWLEDGMENTS

This research was funded, in part, with qualified outer continental shelf oil and gas revenues by the Coastal Impact Assistance Program, U.S. Fish and Wildlife Service, U.S. Department of the Interior. The views and conclusions contained in this document are those of the authors and should not be interpreted as representing the opinions or policies of the U.S. Government. Mention of trade names or commercial products does not constitute their endorsement by the U.S. Government. This research was also funded in part by an Alaska Space Grant Graduate Research Fellowship.

REFERENCES

- Alaska Department of Commerce, Community, and Economic Development 2014. "Quarterly Report: 2014, October-December (Q2) Golovin." Retrieved 01/04/2014 <http://commerce.alaska.gov/cra/DCRAExternal/RUBA/ViewReport/43da147d-dc66-4481-9306-4223c773436f>
- Alaska Center for Climate Assessment and Policy and Scenarios Network for Alaska and Arctic Planning (2014). "Historical sea ice concentration." Retrieved 02/20/2014 <http://seaiceatlas.snap.uaf.edu/explore#location/1850/01/67.00/-162.25/71>
- Buscombe, D., D.M. Rubin, and J. A. Warrick 2010. "A universal approximation of grain size from images of noncohesive sediment." *J. Geophys. Res.*, 115, 17.
- Chapman, R., S.-C., Kim, and D. J. Mark 2009. "Storm-induced water level prediction study for the western coast of Alaska." U.S. Army Corps of Engineers, Coastal and Hydraulics Laboratory.
- Del Rio, L., and J.F. Garcia 2014. "Error determination in the photogrammetric assessment of shoreline changes." *Natural Hazards*, 65(3), 2385-2397. doi: 10.1007/s11069-012-0407-y
- Douglas, D.C., 2010. "Arctic sea ice decline-Projected changes in timing and extent of sea ice in the Bering and Chuckchi Seas." USGS Open File-Report 2010-1176.
- Iowa State University of Technology 2013. "ASOS/AWOS data download." Retrieved from: http://mesonet.agron.iastate.edu/request/download.phtml?network=AK_ASOS
- Kinsman, N.E.M., and M.R. DeRaps 2012. "Coastal hazard field activities in response to the November 2011 Bering Sea storm, Norton Sound, Alaska." Alaska Division of Geological & Geophysical Surveys Report of Investigation, Fairbanks, Alaska.
- Mason, O. K., J.W. Jordan, L. Lestak, and W.F. Manley, 2012. "Narratives of Shoreline Erosion and Protection at Shishmaref, Alaska: The Anecdotal and the Analytical." *Pitfalls of Shoreline Stabilization*, 3, 73-92.
- Pawlowicz, R., B. Beardsley, and S. Lentz 2002. "Classical tidal harmonic analysis including error estimates in MATLAB using T_TIDE." *Comp. Geos.*, 28, 9.
- Roelvink, D., A. Reniers, A.v. Dongeren, J.v. Thiel de Vries, J. Lescinski, and R. McCall 2010. "XBeach Model Description and Manual." Unesco-IHE Institute for Water Education, Deltara and Delft University of Technology (6 ed.).
- Sallenger, A.H., Jr. 2000. "Storm Impact Scale for Barrier Islands." *J. Coastal Res.*, 16(3), 890-895.
- Sanders, B.F., J.E. Schubert, T. Gallien, and M. Shakeri Majd 2013. "Terrestrial laser scanning of anthropogenic beach berms for urban flood defense." Paper presented at the 2013 Fall Meeting American Geophysical Union, San Francisco, California.
- Smith, J., 2014. "Patterns and potential solutions to coastal geohazards at Golovin, Alaska." (Master's thesis), University of Alaska Fairbanks, Fairbanks, Alaska.
- Smith, J.R., N.E.M. Kinsman, and D. Misra 2013. "Using Worldview-2 multispectral bands for shallow water bathymetric survey near Wales, Alaska." Alaska Division of Geological & Geophysical Surveys: American Society of Photogrammetry and Remote Sensing Annual Meeting, Baltimore, Maryland.
- Sorensen, R.M., 2006. *Basic Coastal Engineering*, Springer (3 ed.), New York, New York.
- Southerland, L.E., and N.E.M. Kinsman, 2014. "Lidar data for the community of Golovin, Alaska." Alaska Division of Geological & Geophysical Surveys, Fairbanks, Alaska.
- Stockdon, H.F., R.A. Holman, P.A. Howd, and A.H. Sallenger 2006. "Empirical parameterization of setup, swash, and run-up." *Coast. Eng.*, 53, 573-588.
- Thieler, E.R., E.A. Himmelstoss, J.L. Zichichi, and A. Erugl 2009. "Digital Shoreline Analysis System (DSAS) version 4.0 - An ArcGIS extension for calculating shoreline change." U.S. Geological Survey.
- U.S. Army Corps of Engineers 2009. "Alaska baseline erosion assessment, study findings and technical report." Elmendorf Airforce Base, Alaska.
- U.S. Army Corps of Engineers 2011. "Shaktolik Coastal Flooding Analysis." U.S. Army Corps of Engineers Coastal and Hydraulics Laboratory, Denali Commission, 18 p.
- U.S. Army Corps of Engineers 2013. "Wave Information Studies." Retrieved from <http://wis.usace.army.mil/hindcasts.shtml?dmn=alaskaWIS>.
- U.S. Government Accountability Office 2009. Report to congressional requestors: "Alaska Native villages, limited progress has been made on relocating villages impacted by flooding and erosion."
- U.S. General Accounting Office 2003. "Alaska Native Villages: Most are affected by Flooding and Erosion, but Few Qualify for Federal Assistance."
- Warrick, J.A., D.M. Rubin, P. Ruggiero, J.N. Harney, A.E. Draut, and D. Buscombe 2009. "Cobble cam: grain-size measurements of sand to boulder from digital photographs and autocorrelation analyses." *Earth Surface Processes & Landforms.*, 34, 1811-1821.